N72-19480

NEAR FIELD ANTENNA PATTERNS OF OBSTRUCTED CASSEGRAINIAN TELESCOPES

2nd Interim Progress Report

on

NASA Contract NAS8-25562
DCN 1-0-40-92062 (1F) (S3)

Prepared by

William E. Webb
Project Director

Submitted to

The National Aeronautics and Space Administration
George C. Marshall Space Flight Center
Marshall Space Flight Center, Alabama 35812

University of Alabama
College of Engineering
Bureau of Engineering Research

BER Report No. 143-70

University, Alabama 35486

January, 1972

NEAR FIELD ANTENNA PATTERNS OF OBSTRUCTED CASSEGRAINIAN TELESCOPES

2nd Interim Progress Report

on

NASA Contract NAS8-25562
DCN 1-0-40-92062 (1F) (S3)

Prepared by

William E. Webb
Project Director

Submitted to

The National Aeronautics and Space Administration
George C. Marshall Space Flight Center
Marshall Space Flight Center, Alabama 35812

University of Alabama
College of Engineering
Bureau of Engineering Research

BER Report No. 143-70

University, Alabama 35486

January, 1972

ACKNOWLEDGEMENT

This report was prepared by The University of Alabama under NASA contract number NAS8-25562 (Mod 2), Study of the Effects of Atmospheric Turbulence on Laser Communications Systems, for the George C. Marshall Space Flight Center of the National Aeronautics and Space Administration. This work was administered under the technical direction of the Astrionics Laboratory, George C. Marshall Space Flight Center.

ABSTRACT

The near field antenna pattern of an obstructed optical transmitter, such as a cassegrainian telescope, has been computed using the Fresnel approximation to the scalar diffraction integral. A number of cases have been considered. These include uniformly illuminated, obstructed circular apertures, and apertures coherently illuminated with a divergent gaussian beam wave such as may be obtained from the TEM_{oo} mode of a laser. Other beam profiles that may be derived by energy redistribution of the laser beam have also been considered.

The techniques used for the numerical evaluation of the Fresnel integral are discussed and results for the optical systems to be used on the Marshall Space Flight Center's High Altitude Aircraft Optical Communications Experiment are presented.

TABLE OF CONTENTS

LIST OF FIGURES

INTRODUCTION

The Marshall Space Flight Center's High Altitude Aircraft Test for Visible Laser Optical Communications (AVLOC) will use cassegrainian telescopes as transmitting optics on both the air-to-ground and ground-to-air links.[1] For very long ranges, such as earth to satellite, cassegrainian optics will cause no difficulty provided that collimated or focused beams are used. Under these conditions the shadow of the secondary mirror will be filled with diffracted light and the intensity maximum of the telescope's antenna pattern will lie on the optical axis of the telescope. That is to say that the far field diffraction pattern does not contain the shadow of the central obstruction. Many optical tracking and communication systems, including those employed on the AVLOC experiment, operate over much shorter path lengths so that both receivers are in the near field of their respective transmitters and hence see a doughnut shaped radiation pattern with a dark shadow on the optical axis. Even very long path lengths will not eliminate the central shadow if the transmitted beam has a divergence greater than the beam spreading due to diffraction by the aperture. In the case of divergent beams, one is in effect always in the near field.

Since most optical communications systems require a divergent transmitted beam to keep the pointing errors less than the beam spread, it would appear that some technique must be used to eliminate the central shadow, or else cassegrainian optics (or any other obstructed optical system) cannot be used. One might, for example, offset the transmitted beam with respect to the axis of the tracking system by an angle sufficient to remove the receiver from the dark central portion of the beam. This is undesirable, however, since the inclusion of such a point-ahead angle will complicate the pointing and tracking problems and is also wasteful of the transmitted energy. A more attractive solution would be to reduce the diameter of transmitted beam and displace it laterally from the optical axis of the telescope so that it uses a small transmitter aperture located in the unobstructed portion of the telescope. Other techniques, such as dithering the beam at a high rate to effectively smear it over a large area, or including diffusers in the optical system at appropriate points, might also be considered.

In the case of the AVLOC test, there are two effects which could conceivably make the inclusion of a pointing offset or other technique unnecessary. The ranges to be employed in the experiment are such that the receiver is not located very deep in the Fresnel region. This is especially true of the downlink where the receiver will lie in the transition region between the near and far fields. At these distances there may be enough spreading of the beam by diffraction to provide usable levels of illumination near the axis. In addition atmospheric effects will tend to smear the beam and help to eliminate the central shadow.

The primary purpose of this report is the compute the antenna patterns for the transmitting optics to be used in the AVLOC communications system and to estimate the amount of illumination in the central shadow of the cassegrainian obscuration. The theoretical relations and computer programs developed are quite general however, and can be directly applied to any obstructed optical system. Although other investigators have studied the far field patterns of obstructed optical systems [2], to our knowledge the near field region has never been analyzed.

We have computed the near field diffraction patterns for a cassegrainian telescope system transmitting a coherent gaussian beam. Numerical calculations have been made for a number of ranges and beam divergence angles typical of the conditions which will be encountered during the AVLOC test. Calculations have also been made for shorter ranges representative of the Marshall Space Flight Center Optical Range between Madkin and Bradford Mountains. These calculations were performed for the purpose of comparison with beam profile measurements made by MSFC personnel on the ground transmitter system. In addition we have investigated the near field pattern of an obstructed telescope in which the beam profile has been redistributed by means of an optical axicon. The effect of atmospheric turbulence in helping to fill the central shadow is also considered.

THEORETICAL BACKGROUND

We may consider the diffraction pattern of the cassegrainian telescope as that of a circular aperture containing a central opaque disk and illuminated with a divergent gaussian beam.* Let $U(x_o, y_o)$ be the complex representation of the field at an observation point (x_o, y_o, z) and $U(x_1, y_1)$ be the field at a point $(x_1\ y_1\ o)$ within the aperture, z being the distance between the receiver and transmitter. We also define

- a = radius of the central obstruction
- b = radius of the telescope objective
- λ = wavelength
- k = the propagation number
- P = laser power
- R = radius of curvature of laser beam
- ω = beam width
- θ = beam divergence (half angle)

In the near field, the field distribution of a coherently illuminated aperture is given by the Fresnel approximation [3]

---

*The uplink beam is in fact not gaussian due to the inclusion of an energy redistribution device in the optical system. The effects of the beam redistribution will be considered separately.

$$U_o(x_o,y_o) = \iint_{A'} U_1(x_1,y_1) \frac{e^{jkz}}{j\lambda z} \exp\left\{ \frac{jk}{2z} [(x_1-x_o)^2 + (y_1-y_o)^2] \right\} dx_1 dy_1 \tag{1}$$

where A' is the unobstructed portion of the aperture. We will assume that the laser is operated in the TEM_{oo} mode so that $U_1(x_1,y_1)$ is given by the gaussian beam approximation

$$U_1(x_1,y_1) = \sqrt{\frac{2P}{\pi\omega^2}} \exp\left[\frac{jkr_1^2}{2R} - \frac{r_1^2}{\omega^2} \right] \tag{2}$$

where $r_1^2 = x_1^2 + y_1^2$. The factor $(2P/\pi\omega^2)^{1/2}$ is included so that $|U|^2$ will be the illuminance in watts per square meter. Substituting equation 2 into equation 1 and converting to polar coordinates we obtain

$$U_o(r_o,\theta_o) = \frac{1}{\lambda z} \sqrt{\frac{2P}{\pi\omega^2}} \int_0^{2\pi} \int_a^b \exp\left[jk \frac{r_1^2}{2R} \right] \exp\left[- \frac{r_1^2}{\omega^2} \right]$$

$$\exp\left[\frac{jk}{2z} [r_1^2 + r_o^2 - 2r_1 r_o \cos(\theta_1-\theta_o)] \right] r_1 dr_1 d\theta_1 \tag{3}$$

A phase factor $-je^{-jkz}$ has been dropped from equation 3 since it will not effect the intensity $I = |U_o|^2$. It should also be noted that contrary to common usage ω is the distance at which the field, rather than the intensity, falls to 1/e of its maximum value and that the signs in the exponents have been chosen to make R positive for divergent beams instead of for focused beams. We now apply a well known integral representation for the Bessel Function.

$$J_o(\xi) = \frac{1}{2\pi} \int_0^{2\pi} \exp\{-j\ \xi \cos(\theta-\phi)\}\, d\theta \tag{4}$$

to obtain

$$U_o(r_o) = \frac{2\pi}{\lambda z} \sqrt{\frac{2P}{\pi\omega^2}} \int_a^b \exp\{\frac{-r_1^2}{\omega^2}\} \exp\{j\ \frac{k}{2}\ (\frac{1}{R} + \frac{1}{z})\ r_1^2\}\ J_o(\frac{kr_1r_o}{z})\ r_1 dr_1 \tag{5}$$

Again a phase factor which will not influence the intensity has been omitted.

Equation 5 is the Fresnel Diffraction pattern for an obscured aperture illuminated by a gaussian beam and is valid for all ranges likely to be of interest in optical communications. The persistence of the central shadow for large values of z can be understood by inspection of equation 5. Consider for a moment the case of a collimated beam. The radius of curvature of the beam is infinite and equation 5 reduces to

$$U(r_o) = \frac{2\pi}{\lambda z} \sqrt{\frac{2P}{\pi\omega^2}} \int_a^b \exp\{\frac{-r_1^2}{\omega^2}\} \exp\{j\ \frac{k}{2z}\ r_1^2\}\ J_o\{\frac{kr_1r_o}{z}\}\ r_1 dr_1 \tag{6}$$

for z small $U_o(r)$ must approach the geometrical optics limit of a gaussian beam with sharp central and peripheral shadows. However, for large z the term $\{\frac{jkr_1^2}{2z}\}$ vanishes and equation 6 further reduces to the well known Fraunhoffer approximation

$$U(r_o) = \frac{2\pi}{\lambda z} \sqrt{\frac{2P}{\pi\omega^2}} \int_a^b \exp\{\frac{-r_1^2}{\omega^2}\}\ J_o\{\frac{kr_1r_o}{z}\}\ r_1 dr_1 \tag{7}$$

which has an intensity maximum at $r_o = 0$. Thus the condition for the elimination of the central shadow for a collimated beam is that

$$z >> \left|\frac{kr_1^2}{2}\right|_{max.} \tag{8}$$

i.e., the range must be great enough to place the observer well into the far field. Now for the case of an uncollimated beam this condition becomes

$$\frac{1}{R} + \frac{1}{Z} << \left|\frac{2}{kr_1^2}\right|_{min.} \tag{9}$$

If the beam is converging the Fraunhoffer condition is satisfied near the focus (R = -Z). However, if R is small and positive, as it is for a divergent beam, the inequality of equation 9 cannot be satisfied for any value of Z, no matter how large. Hence one is in effect always in the near field and the central shadow will be observed at all ranges. For R small compared to Z equation 9 may be written as

$$R >> \left|\frac{kr_1^2}{2}\right|_{max} \tag{10}$$

or

$$R >> \frac{kb^2}{2}$$

which corresponds to a beam divergence half angle of

$$\theta_m < \frac{2}{kb} \tag{11}$$

Here θ_m is the largest beam divergence for which the central shadow will disappear at long ranges.

The preceding result may be interpreted physically as follows. For a divergent beam the geometric shadow of the central obscuration is a cone with it's apex located at the center of curvature of the wave front and a half angle θ. Light from the unobscured part of the aperture will be spread by diffraction; the angular divergence due to diffraction being of the order of λ/b. If θ is less than λ/b then for large distances the light will eventually fill the central shadow, however, if θ is greater than λ/b the spreading due to diffraction is not great enough to compensate for the beam divergence and the shadow is never illuminated.

ON AXIS ILLUMINANCE

On the z axis equation 5 takes a particularly simple form since here $r_o = 0$ and $J\left(\frac{k\, r_1 r_o}{z}\right) = 1$. Then

$$U_o(0) = \frac{k}{z}\sqrt{\frac{2P}{\pi\omega^2}} \int_a^b e^{-\alpha r_1^2} r_1 dr_1 \qquad (12)$$

where

$$\alpha = \frac{-1}{\omega^2} + j\,\frac{k}{2}\left(\frac{1}{R} + \frac{1}{z}\right) \qquad (13)$$

It will be useful to investigate the on axis illuminance since it will provide a check on the accuaracy of the numerical integration needed to evaluate the off axis intensity. Equation 12 may be integrated directly to yield

$$U_o(0) = \frac{k}{z}\sqrt{\frac{2P}{\pi\omega^2}}\ \frac{1}{2\alpha}\left[e^{+\alpha b^2} - e^{-\alpha a^2}\right] \qquad (14)$$

The intensity along the axis is then given by

$$I(0) = |U_o(0)|^2 \qquad (15)$$

$$I(0) = \frac{k^2}{4z^2|\alpha|^2}\ \frac{2P}{\pi\omega^2}\ \left(e^{\alpha b^2} - e^{\alpha a^2}\right)\left(e^{\alpha^* b^2} - e^{\alpha^* a^2}\right) \qquad (16)$$

which reduces to

$$I(0) = \frac{k^2 P}{2\pi\ z^2 |\alpha|^2 \omega^2} [\ e^{(\alpha + \alpha^*) b^2} + e^{(\alpha + \alpha^*) a^2}$$

$$- e^{(\alpha a^2 + \alpha^* b^2)} - e^{(\alpha^* a^2 + \alpha b^2)}] \tag{17}$$

$$I(0) = \frac{k^2 P}{2\pi\ z^2 |\alpha|^2 \omega^2} [\ e^{2\mathrm{Re}\alpha a^2} + e^{2\mathrm{Re}\alpha b^2}$$

$$- 2e^{\mathrm{Re}\alpha (a^2 + b^2)} \cos(\mathrm{Im}\alpha (a^2 - b^2))] \tag{18}$$

$$I(0) = \frac{2P}{\pi\omega^2 [(1 + \frac{z}{R})^2 + \frac{4z^2}{k^2 \omega^4}]} \quad e^{-2\frac{b^2}{\omega^2}} + e^{-\frac{2a^2}{\omega^2}}$$

$$- 2e^{-\frac{a^2 + b^2}{\omega^2}} \cos [\ \frac{k}{2} (\frac{1}{R} + \frac{1}{z}) (a^2 - b^2)] \tag{19}$$

The first exponential terms in equation 19 arise from the loss of the center portion of the beam from obscuration by the cassegrainian secondary and the loss of the tails of the beam at the objective. The harmonic term is due to the changing number of Fresnel zones contained within the aperture as one moves along the axis. This result is the alternating maxima and minima in the intensity along the axis characteristic of Fresnel diffraction.

For the ranges to be used in the AVLOC experiment $z/R >> 1$ and $(2z/k\omega^2) << 1$. Equation 19 then simplifies to

$$I(0) = \frac{2P}{\pi\omega^2 z^2/R^2}\Big[e^{-2(b/\omega)^2} + e^{-2(a/\omega)^2} - 2e^{-(a^2+b^2)/\omega^2} \cos\{\frac{k}{2}(\frac{1}{R}+\frac{1}{z})(a^2-b^2)\}\Big] \tag{20}$$

But since

$$\theta = \omega/R \tag{21}$$

and $\pi(z\theta)^2$ is just the geometrical area of the beam in the receiver plane we may let $I'(0)$ denote the intensity which one would compute neglecting the central obstruction, the gaussian beam shape and all diffraction effects. Then

$$I(0) = I'(0)\ 2(e^{-2(a/\omega)^2} + e^{-2(b/\omega)^2} - 2e^{-(a^2+b^2)/\omega^2} \cos(\frac{k}{2}(\frac{1}{R}+\frac{1}{z})(a^2-b^2)) \tag{22}$$

Clearly I (0) will have maxima and minima when the cosine term is ±1. Then

$$I_{max/min} = I' \cdot 2(e^{-(a/\omega)^2} \pm e^{-(b/\omega)^2})^2 \tag{23}$$

If we choose $\omega = b$ and $a = b/3$ then $I_{max} = 3.18\ I'$ and $I_{min} = 0.55\ I'$, or a factor of about 6 to 1 difference in intensity. If one is going to work on axis it would be worthwhile to choose the aircraft range so as to take advantage of the maxima. The ability to do this depends, of course, upon the spacing of the maxima being great enough to allow the aircraft to remain near the maxima rather than fluctuating between maxima and minima. We may estimate this spacing by noting that maxima will occur when

$$\frac{k}{2}\left(\frac{1}{z}+\frac{1}{R}\right)(b^2 - a^2) = (2n + 1)\ \pi \tag{24}$$

n being an integer. Solving for z we obtain

$$Z_m = \left[\frac{(2n + 1)\ \lambda}{(b^2 - a^2)} - \frac{1}{R}\right]^{-1} \tag{25}$$

or

$$\Delta Z_m = \frac{1}{\left[\frac{(2n+1)\lambda}{(b^2-a^2)} - \frac{1}{R}\right]} - \frac{1}{\left[\frac{(2n+3)\lambda}{(b^2-a^2)} - \frac{1}{R}\right]} \tag{26}$$

$$\Delta Z_m = Z_m - \frac{1}{\left[1/Z_m + \frac{2\lambda}{b^2 - a^2}\right]} \tag{27}$$

$$\Delta Z_m = \frac{2\lambda\ Z_m^{\ 2}}{(b^2 - a^2)} \Big/ \left(1 + \frac{2\lambda\ Z_m}{(b^2 - a^2)}\right) \tag{28}$$

but $2\lambda\ Z_m/(b^2 - a^2) << 1$, therefore

$$\Delta Z_m = \frac{2\lambda\ Z_m^{\ 2}}{b^2 - a^2} \tag{29}$$

We choose a = 10 cm, b = 30 cm, λ = 6328 Å and Z = 20 km. ΔZ then is of the order of 6 km. so that the variation of I(0) with Z is clearly slow enough to allow the aircraft to remain near a maximum. Inspection of equation 25 shows that while the spacing between maxima is independent of R their position is not. Since R can be controlled by adjusting the beam divergence θ it should be possible to locate the receiver near an axis illuminance maxima for both the uplink and downlink beams.

The on axis illuminance which we have computed corresponds to the bright central spot usually observed in the Fresnel diffraction from an opaque disk [6]. The question remains whether or not this spot is broad enough to provide usable powers. In order to answer this question it is necessary to investigate the variation of illuminance with the distance off axis.

ILLUMINANCE OFF AXIS

The illuminance at a point off axis is given from equation 5

$$I(r_o,z) = \frac{2P}{\pi\omega^2}\left(\frac{k}{z}\right)^2 (S^2 + C^2) \tag{30}$$

where

$$S = \int_a^b e^{-(r/\omega)^2} J_o\left(\frac{kr_1r_o}{z}\right) \cdot \sin(\beta r_1^{\,2})\ r_1dr_1 \tag{31}$$

and

$$C = \int_a^b e^{-(r/\omega)^2} J_o\left(\frac{kr_1r_o}{z}\right) \cos(\beta r_1^{\,2})\ r_1dr_1 \tag{32}$$

$$\beta = \frac{k}{2}\left(\frac{1}{R} + \frac{1}{z}\right) \tag{33}$$

The evaluation of S and C is relatively difficult since the argument of the Bessel function is such that neither the asymptotic nor ascending power expansions coverage rapidly. Furthermore, the trigonometric functions oscillate so rapidly that numerical integrating requires a very large number of points to accurately sample the function. This in turn requires that the integrand be evaluated with high precision to avoid an unacceptable accumulation of round off errors. Several methods of evaluating C and S were considered, including an expansion by repeated integration by parts leading to a series of Bessel functions of increasing order and fixed argument. This series, which resembles the classical Lommel function expansion, was so weakly convergent that it proved to be even less efficient than direct numerical integration.

The method finally chosen for the evaluation of S and C was a Simpson's Rule integration with two correction terms. The zero order Bessel function was computed using an ascending power series [4]

$$J_o(\xi) = \sum_{r=o}^{\infty} (-1)^r \frac{(\frac{1}{2}\xi)^{2r}}{(r!)^2} \tag{34}$$

for values of ξ less than 10 and Hankel's asymptotic expansion [5]

$$\underset{\xi \to \infty}{J_o(\xi)} = \sqrt{\frac{2}{\pi\xi}} \{P(\xi) \cos \chi + Q(\xi) \sin \chi\} \tag{35}$$

$$P = 1 - \frac{3^2}{2!(8\xi)^2} + \frac{3^2 \cdot 5^2}{4!(8\xi)^4} - - - - \tag{36}$$

$$Q = \frac{-1}{8\xi} + \frac{1 \cdot 3^2 \cdot 5^2 \cdot 7^2}{3!(8\xi)^3} - \ldots \tag{37}$$

$$\chi = \xi - \pi/4 \tag{38}$$

for ξ greater than 10. Double precision arithmetic was used throughout.

We have investigated the errors in the numerical integration, both by consideration of the error in the calculation of the integrand, by examining the magnitude of the correction terms in the Simpson's Rule algorithm, and by varying the number of points used in the integration. It is concluded that the maximum error will not exceed 0.1%. Furthermore, it was found that the value of $I(0)$ calculated from equation 30 agrees very closely with that found from equation 22.

The computer programs used for these calculations are described in Appendix A.

EFFECTS OF ENERGY REDISTRIBUTION

In the previous sections the field distribution in both the ground-based and airborne transmitting apertures was assumed to be a truncated gaussian beam mode. The ground based telescope in fact will not have a gaussian intensity distribution in the exit pupil since it contains a device, called an axicon, which redistributes the beam in such a way that all the energy in the beam is incident upon the unobscured portion of the aperture. For the purpose of estimating the order of magnitude of the illuminance near the axis the truncated gaussian approximation was adequate. It is desirable, however, to be able to compare the theoretical diffraction patterns with beam profiles observed over relatively short horizontal paths. In this way estimates of atmospheric spreading of the beam may be obtained. For this purpose it will be necessary to consider the effect of the energy redistribution of the near field pattern.

Two possible physical realizations of the axicon are shown in figure 1. The axicon shown in Fig. 1a displaces the beam outward in a radial direction producing an energy distribution in the exit pupil usually referred to as a "displaced gaussian" distribution. The axicon illustrated in Fig. 1b not only displaces the energy outward from the optical axis but also inverts the intensity distribution in the sense that light from the center of the entrance pupil is routed to the outside of the exit pupil and visa-versa. This type of

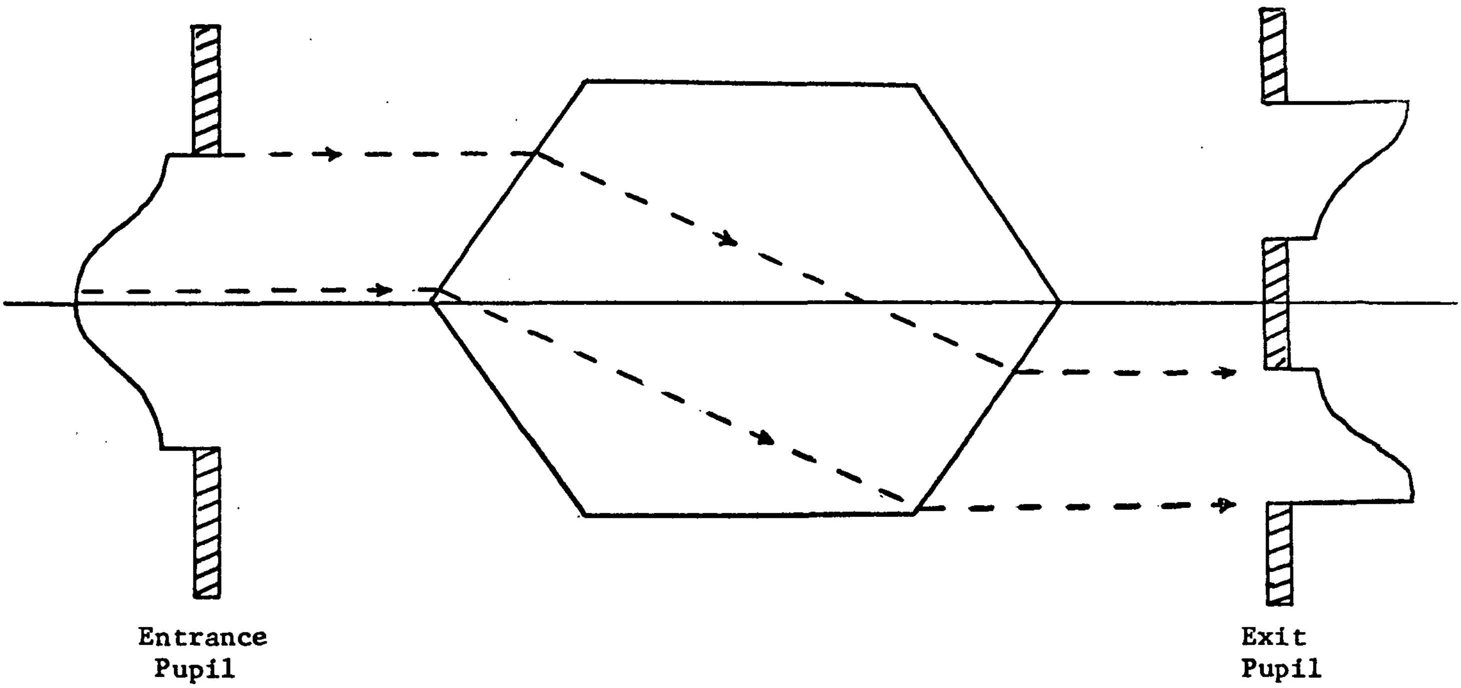

a. plandromic gaussian

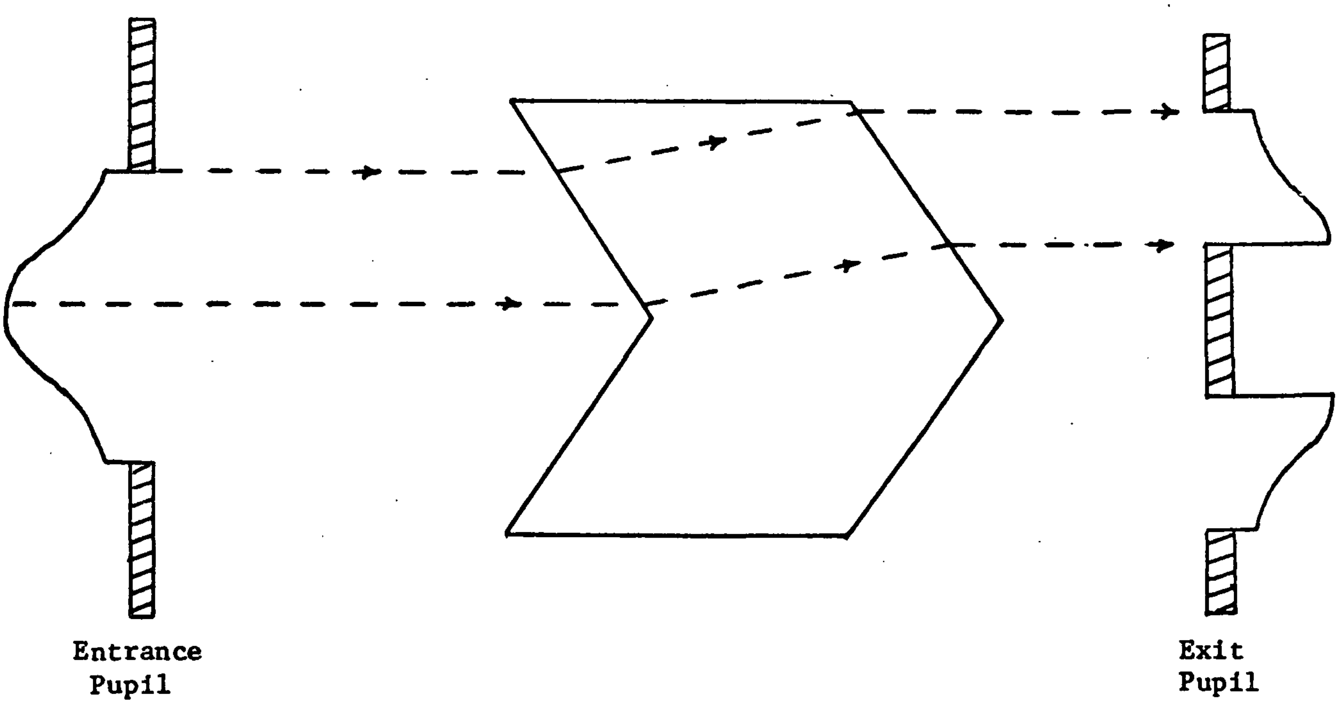

b. displaced gaussian

Figure 1. Two Axicon Devices.

axicon produces an intensity distribution which has been described as "plaindromic gaussian".

We assume that the energy redistribution device in the ground based telescope acts as a plaindromic axicon [7] i.e., it maps the energy contained in an annulus of radius r' in the entrance pupil of the optical system into an annulus of radius r in the exit pupil as shown in Fig. 2a. The radii of the two annuli are related by

$$r = b - \frac{b - a}{T} r' \tag{39}$$

and T is the truncation point of the original beam. This equation is equivalent to Peters and Ledger's equation (9) (reference 7) except that we have allowed an arbitrary truncation point for the original beam while Peters and Ledger have considered only beams which are truncated at a distance equal to the radius of the inner obscuration. Our results are therefore more general in that it will allow for an axicon with a lateral magnification different from unity.

The redistributed beam profile is obtained from the mapping equation (equation 39) and from the conservation of energy.

$$E_p(r) \cdot 2\pi r dr = E_g(r') \cdot 2\pi r' dr' \tag{40}$$

where E_p and E_r are the plaindromic distribution in the exit pupil and gaussian distribution in the entrance pupil respectively. Noting that $E = |U|^2$ we have

$$|U_p(r)| = \left(\frac{r'dr}{rdr}\right)^{1/2} |U_g(r')| \tag{41}$$

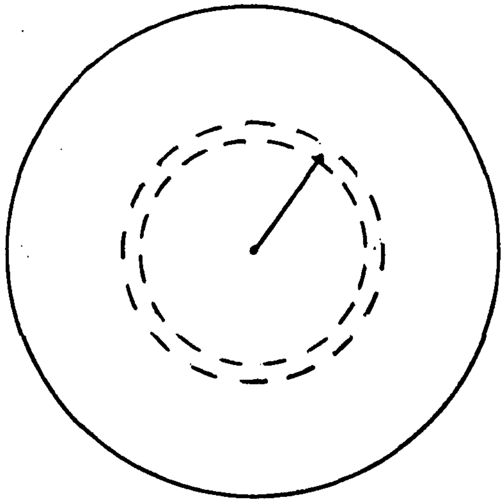

a. entrance pupil

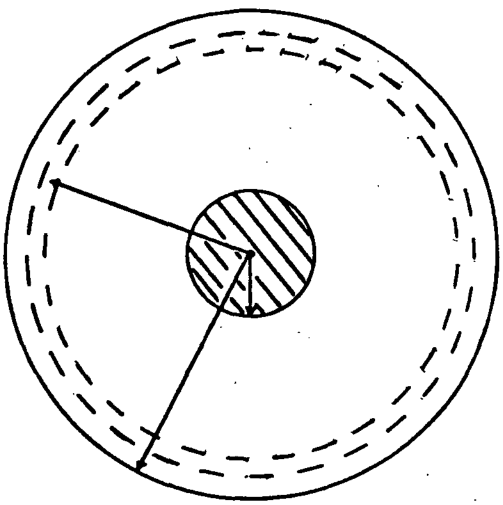

b. exit pupil
plandromic gaussian

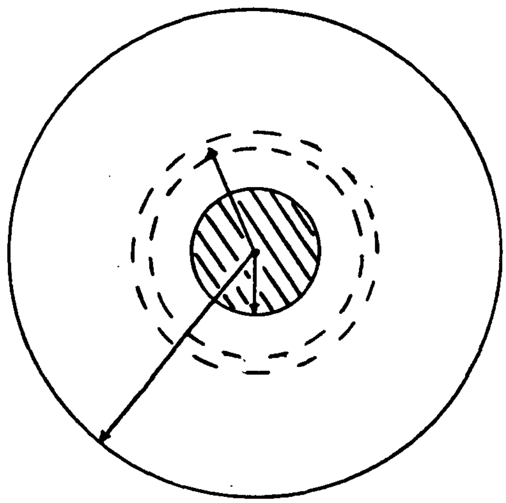

c. exit pupil
displaced gaussian

Figure 2. Energy Mappings for Plandromic and Displaced Gaussian Axicons.

$$|U_p(r)| = \left(\frac{T}{b - a}\right)\left(\frac{b - r}{r}\right)^{1/2} \exp\left\{-\left(\frac{T}{\omega(b - a)}\right)^2 (b - r)^2\right\} \tag{42}$$

Assuming that the beam wave fronts are approximately spherical we may add a phase term and a normalization constant to obtain

$$U_p(r) = \left(\frac{2P}{\pi\omega^2}\right)^{1/2} \frac{T}{b - a} \left(\frac{b - r}{r}\right)^{1/2} \exp\left\{-\left(\frac{T}{\omega(b - a)}\right)^2 (b - r)^2\right\}$$

$$\exp\left\{j \frac{k}{2R} r^2\right\} \tag{43}$$

Equation 43 is now substituted into equation 1 and following the same procedure as before we obtain the equivalent forms of equations 30-34, viz.

$$I(r_o, z) = \frac{2P}{\pi\omega^2} \left(\frac{T}{b - a}\right)^2 \left(\frac{k}{z}\right)^2 (S_p^{\,2} + C_p^{\,2}) \tag{44}$$

where

$$S_p = \int_a^b \left(\frac{b - r_1}{r_1}\right)^{1/2} e^{-\alpha^2 (b - r_1)^2} J_o\left(\frac{kr_1 r_o}{z}\right) \sin(\beta r_1^{\,2})\, r_1 dr_1 \tag{45}$$

and

$$C_p = \int_a^b \left(\frac{b - r_1}{r_1}\right)^{1/2} e^{-\alpha^2 (b - r_1)^2} J_o\left(\frac{kr_1 r_o}{z}\right) \cos(\beta r_1^{\,2})\, r_1 dr_1 \tag{46}$$

α and β given by

$$\beta = \frac{k}{2}\left(\frac{1}{R} + \frac{1}{z}\right) \qquad \alpha = \frac{T}{\omega}/(b - a) \tag{47}$$

Similar expressions can be obtained for a displaced gaussian. In this case equation 37 is replaced by the mapping

$$r = a + \frac{b - a}{T} r' \tag{48}$$

and the remainder of the derivation follows as before. The diffraction pattern from a displaced gaussian is then given by equation (44) with S_p and C_p replaced by S_D and C_D where

$$S_D = \int_a^b \left[\frac{a + r_1}{r_1}\right]^{1/2} e^{-\alpha^2 (a + r_1)^2} J_o\left(\frac{kr_1 r_o}{z}\right) \sin(\beta r_1^2)\, r_1 dr_1 \tag{49}$$

and

$$C_D = \int_a^b \left[\frac{a + r_1}{r_1}\right]^{1/2} e^{-\alpha^2 (a + r_1)^2} J_o\left(\frac{kr_1 r_o}{z}\right) \cos(\beta r_1^2)\, r_1 dr_1 \tag{50}$$

Numerical calculations have been made for a number of ranges and divergence using a plaindromic gaussian distribution and a displaced gaussian distribution. The numerical techniques employed were identical to those used for a gaussian distribution except for the choice of the input function. These results are presented in the following sections.

RESULTS

Numerical calculations have been made for the optical communications systems which will be used by the Marshall Space Flight Center's High Altitude Aircraft Optical Communications Experiment (AVLOC). For the ground to air system the transmitter is a 24 inch (61 cm) diameter cassegrainian telescope with an 8 inch (20 cm) diameter central obstruction. The aircraft to ground system employs a 4 inch (10 cm) telescope with a 1 inch (2.54 cm) obstruction. The transmitted powers and wavelengths are 1 watt at 5880 nm. uplink and 5 milliwatts at 632.8 nm. downlink. Ranges from 50,000 feet (15 Km) to 150,000 feet (45 Km) and beam divergence angles from 0 to 150 arc seconds were considered. The parameters for a typical set of calculations are shown in Table I.

Table I

System	Diameter (in) Aperture	Secondary	Beam Power Watts	Range 1000 ft.	Beam Divergence* Arc Seconds
uplink	24	8	1	80	0
uplink	24	8	1	80	25
uplink	24	8	1	80	50
downlink	4	1	.005	80	25
downlink	4	1	.005	80	50
downlink	4	1	.005	80	75

*half angle

The assumed range (80,000 feet) corresponds to an aircraft approximately 10 miles from the ground station at an altitude of 60,000 feet. For the purpose of these calculations we have assumed a gaussian beam whose beam width equals the outer diameter of the aperture. While this is not the optimum matching to the aperture, it is an adequate approximation, as the final results are not very sensitive to changes in the truncation point except for small changes in the overall amplitude.

The results of these calculations are shown in Figs. 2-8 along with the geometrical optics approximation to the gaussian beam. The geometrical optics approximation was obtained by scaling the beam profile by the relation

$$r_o = \frac{Z + R}{R} r_1 \tag{51}$$

For the uplink beam the diffraction pattern shows the characteristic monotonic decrease of intensity within the geometrical shadows, indicating that one will be deep within the Fresnel region as expected. Examination of the uplink beam patterns indicate that the intensities within the shadow may be expected to be quite low. Furthermore it seems unlikely that smearing by the atmosphere will be sufficient to produce usable illumination in the shadow. In each of these patterns the central maximum (Fresnel-Arago bright Spot) is clearly visible. With the exception of the collimated beam it is far too narrow, however, to be of much use in a practical communications system.

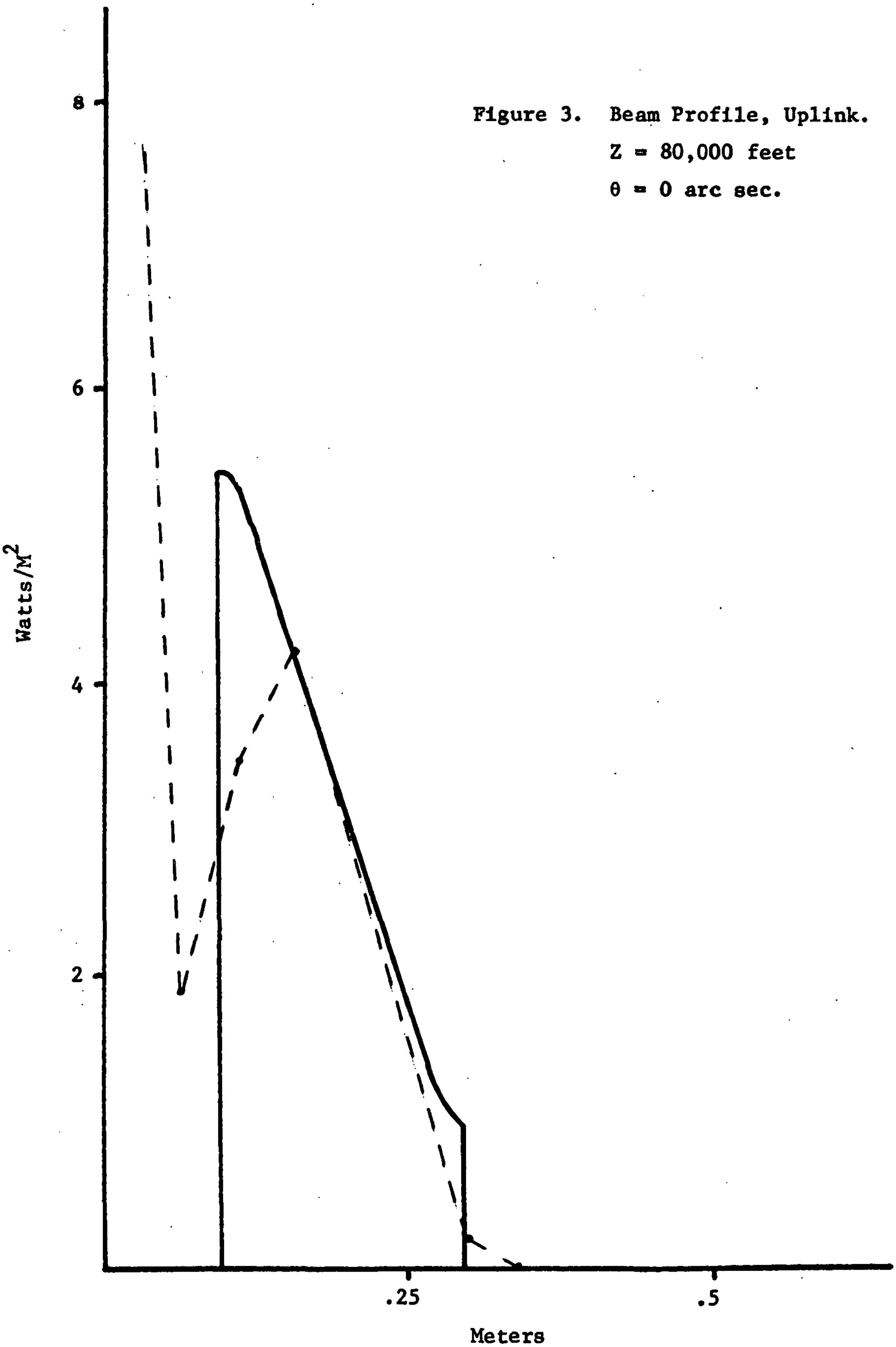

Figure 3. Beam Profile, Uplink.
$Z = 80,000$ feet
$\theta = 0$ arc sec.

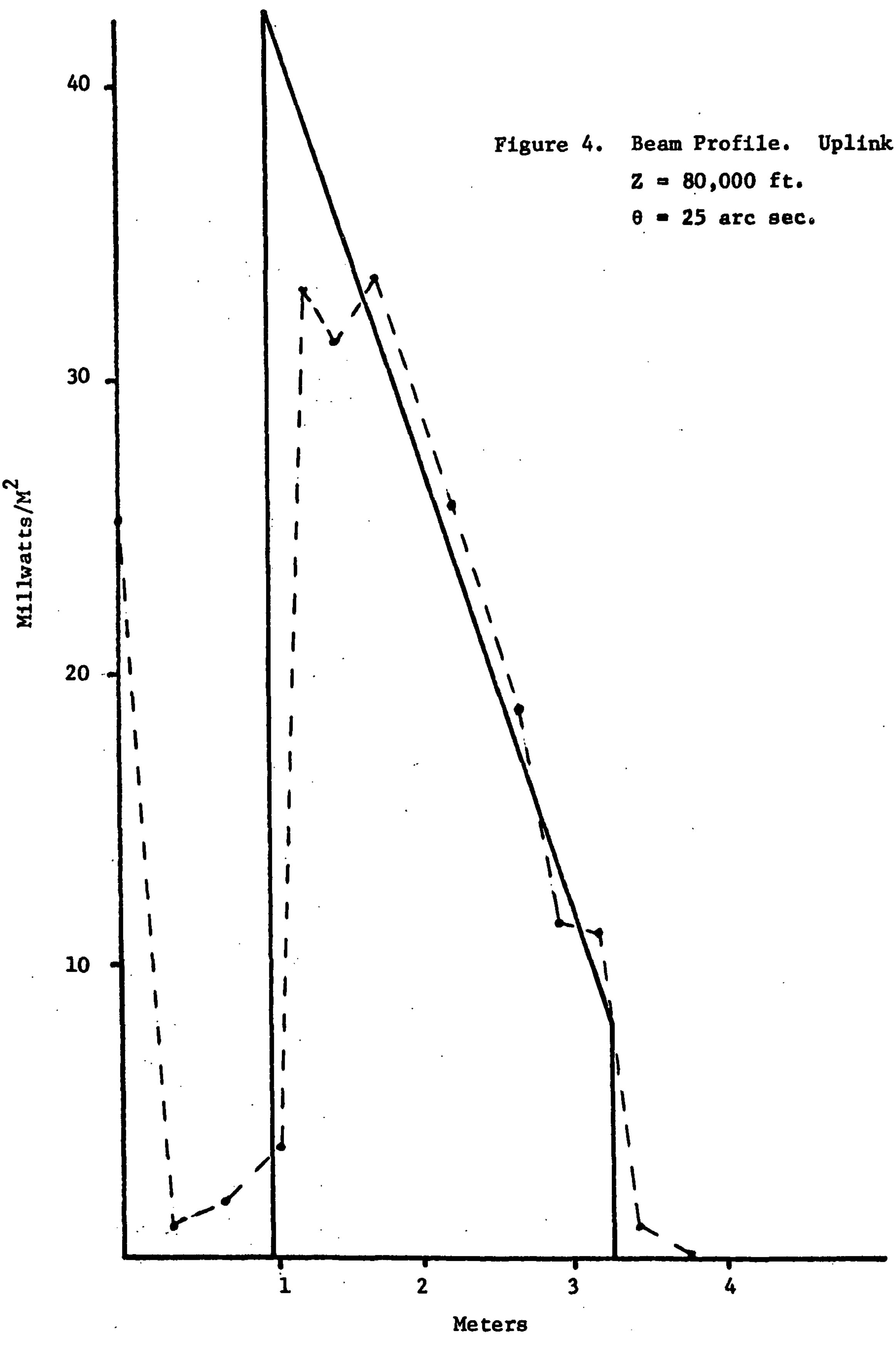

Figure 4. Beam Profile. Uplink
$Z = 80{,}000$ ft.
$\theta = 25$ arc sec.

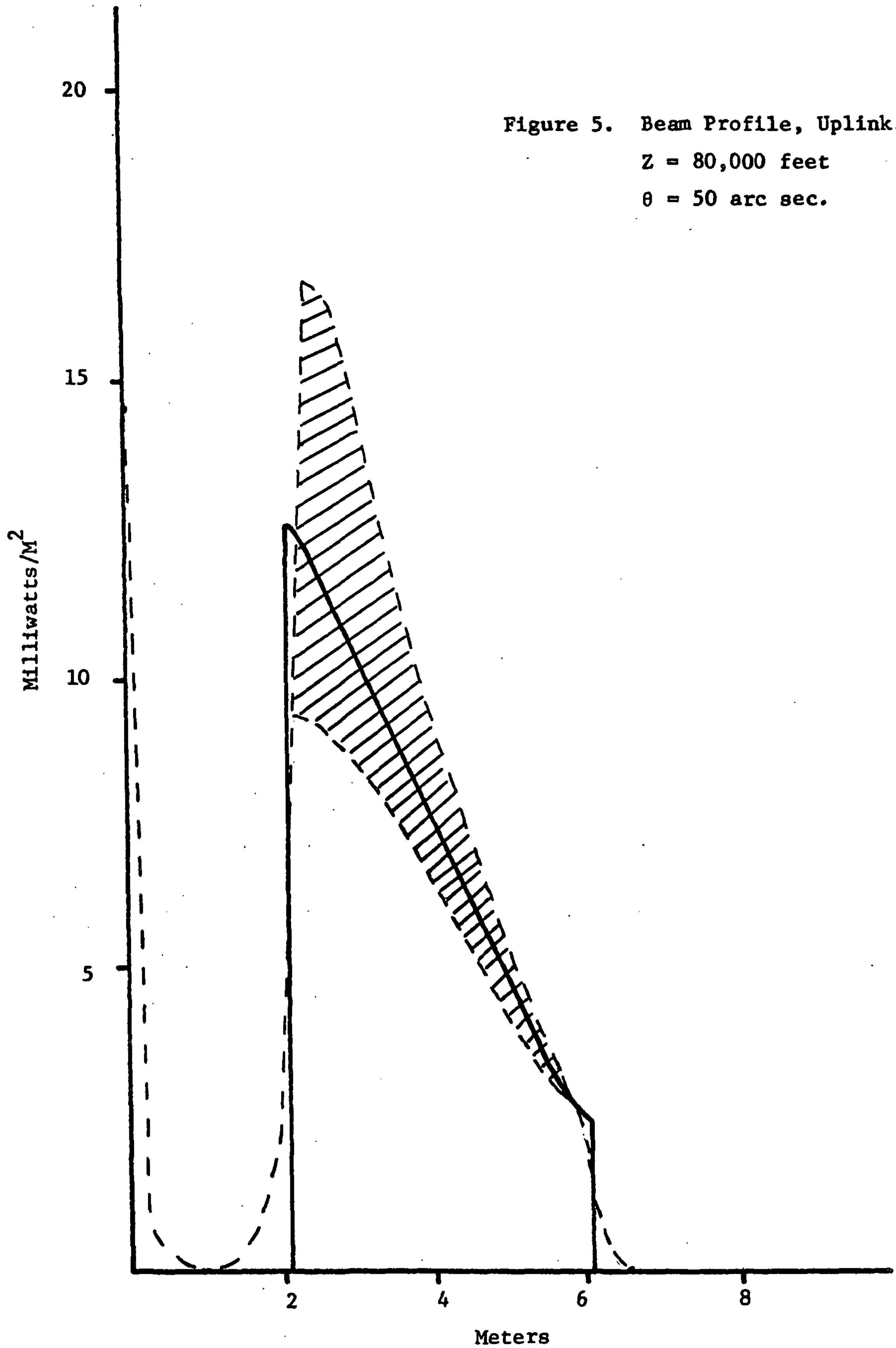

Figure 5. Beam Profile, Uplink.
Z = 80,000 feet
θ = 50 arc sec.

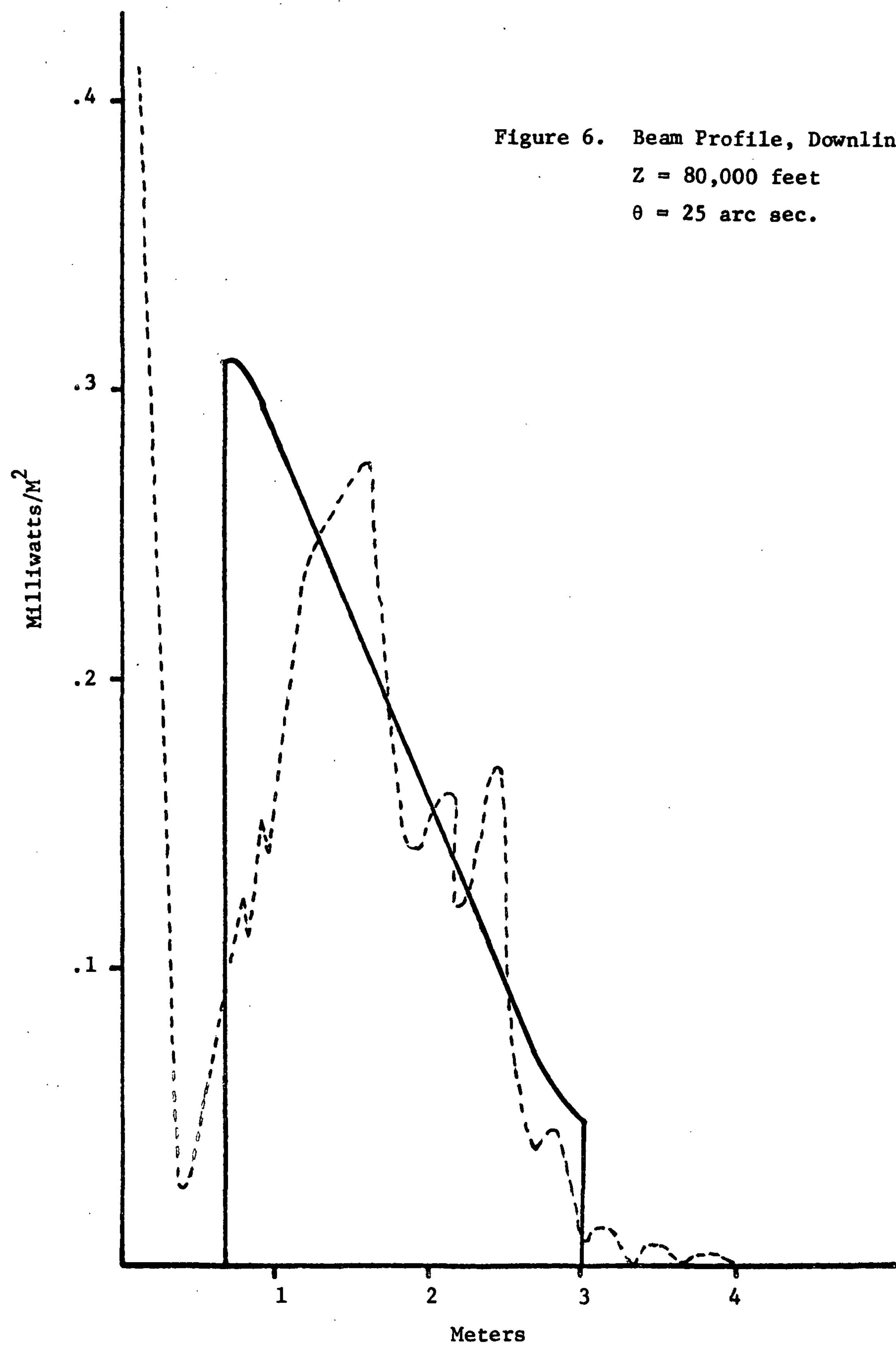

Figure 6. Beam Profile, Downlink.
$Z = 80{,}000$ feet
$\theta = 25$ arc sec.

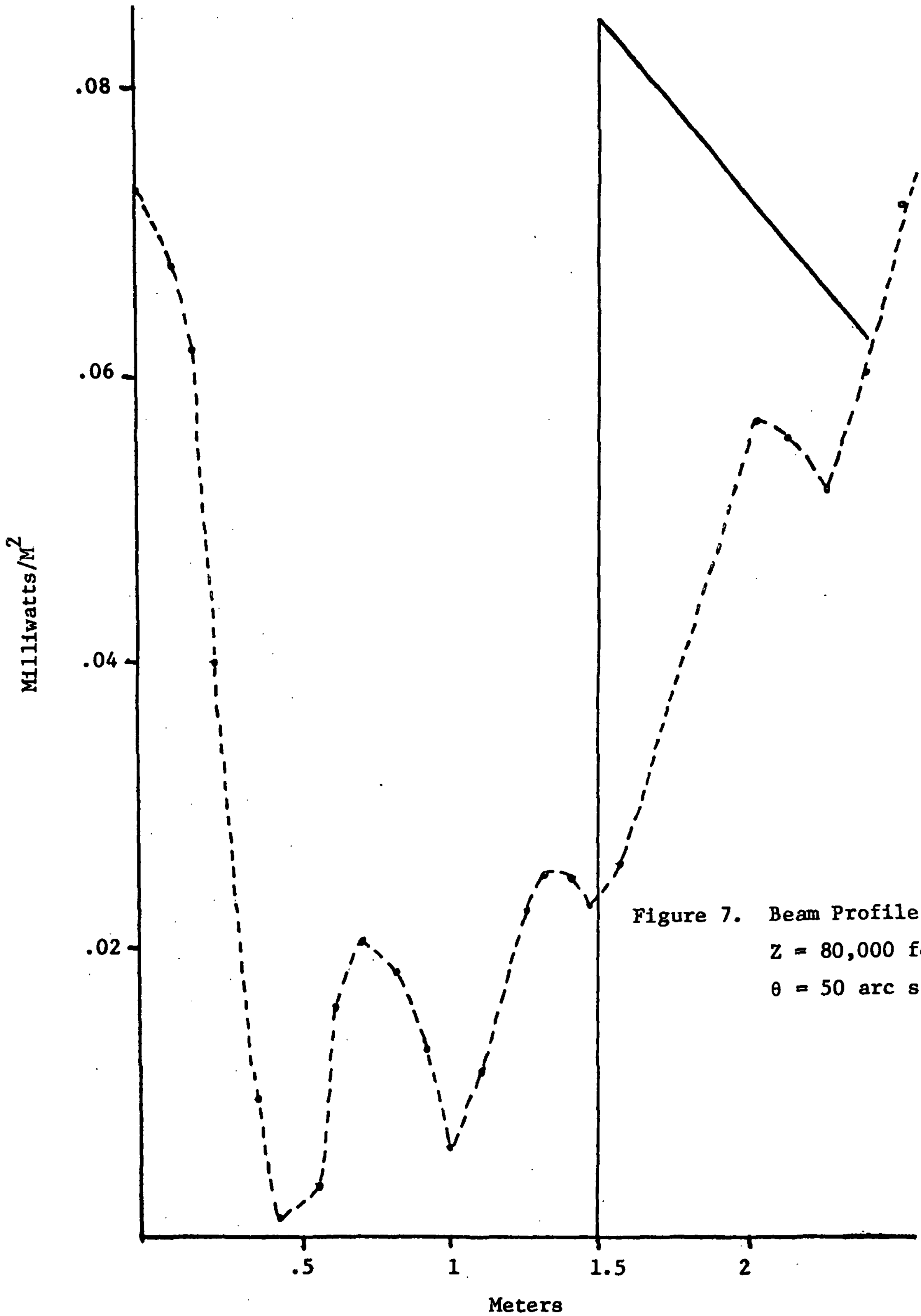

Figure 7. Beam Profile, Downlink.
Z = 80,000 feet
θ = 50 arc sec.

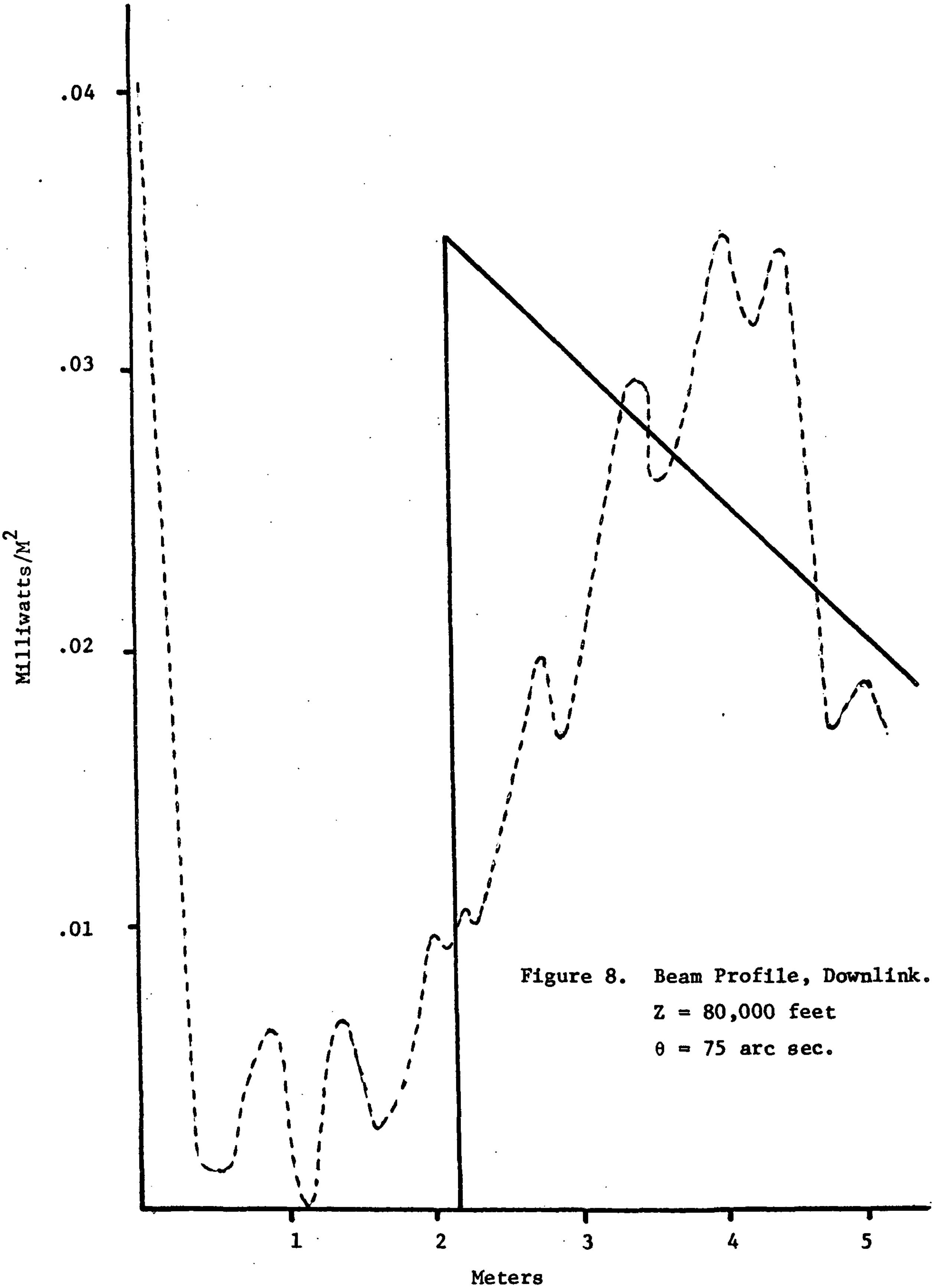

Figure 8. Beam Profile, Downlink.
$Z = 80{,}000$ feet
$\theta = 75$ arc sec.

For larger beam divergence angles, the solution tended to oscillate very rapidly in the directly illuminated region. This behavior was also observed at shorter ranges for smaller values of beam divergence. An example of this can be seen in Fig. 3 where the oscillation was so rapid that it could not be plotted. We have therefore indicated the limits of oscillation by the shaded area. This oscillation was at first a cause of considerable concern as we feared that it might be a spurious result due to error buildup in the computer calculations. A number of tests were made, however, which convinced us that the oscillation does correspond to real fluctuations of the Fresnel pattern. These tests included the following:

1) Computing the intensity at very closely spaced points for one case. When this was done it was found that the fluctuations were smooth oscillations rather than random variations which might be expected from error buildups.

2) The number of points used in the Simpson's rule of integration was varied. It was found that the change in computed intensity due to changing the number of field points was much less than the magnitude of the oscillation.

3) A gaussian integration algorithm was used to compute a few field points. These agreed closely with the results of the Simpson's Rule integration.

4) In all cases the magnitude of the oscillation was greatest for shorter distances of axis. This is the region where the integration algorithm should be the most accurate.

5) No oscillation was observed in the shadow.

The rapid oscillation is of no importance as it will be obliviated by atmospheric effects.

For the downlink the situation is somewhat improved. As can be seen from Figures 5-8 the intensity in the shadow oscillates, indicating that at the assumed range one is approaching the Fraunhoffer region. The central maximum has broadened and the intensity levels near the axis have increased. Since the calculated pattern will be further spread by atmospheric effects and by effects such as tracking system jitter it is expected that usable levels of illuminance will be found near the center of the pattern without additional beam spreading or pointing offsets.

Results at ranges other than 80,000 feet were qualitatively similar. As would be expected the filling of the central decreased at shorter ranges and increased somewhat at longer ranges. There was very little significant difference in the shape of the diffraction pattern at any of the distances considered however. Calculations made with plaindromic and displaced gaussian distributions displaced a somewhat different shape radiation pattern in the directly illuminated region but no significant differences in the fields within the shadows.

We have also calculated the transmitter antenna patterns for the 24 inch cassegrainian telescope at a range of 26,400 feet (8.15 Km), corresponding to the length of the Marshall Space Flight Center Optical Range between Madkin and Bradford Mountains. These calculations were made so that MSFC personnel could compare the actual antenna patterns of the ground based transmitter with the predicted pattern. Two representative patterns are shown in Figures 9 and 10. The beam divergences are 12.5 and 25 arc seconds respectively and a plaindromic gaussian beam was assumed in both cases.

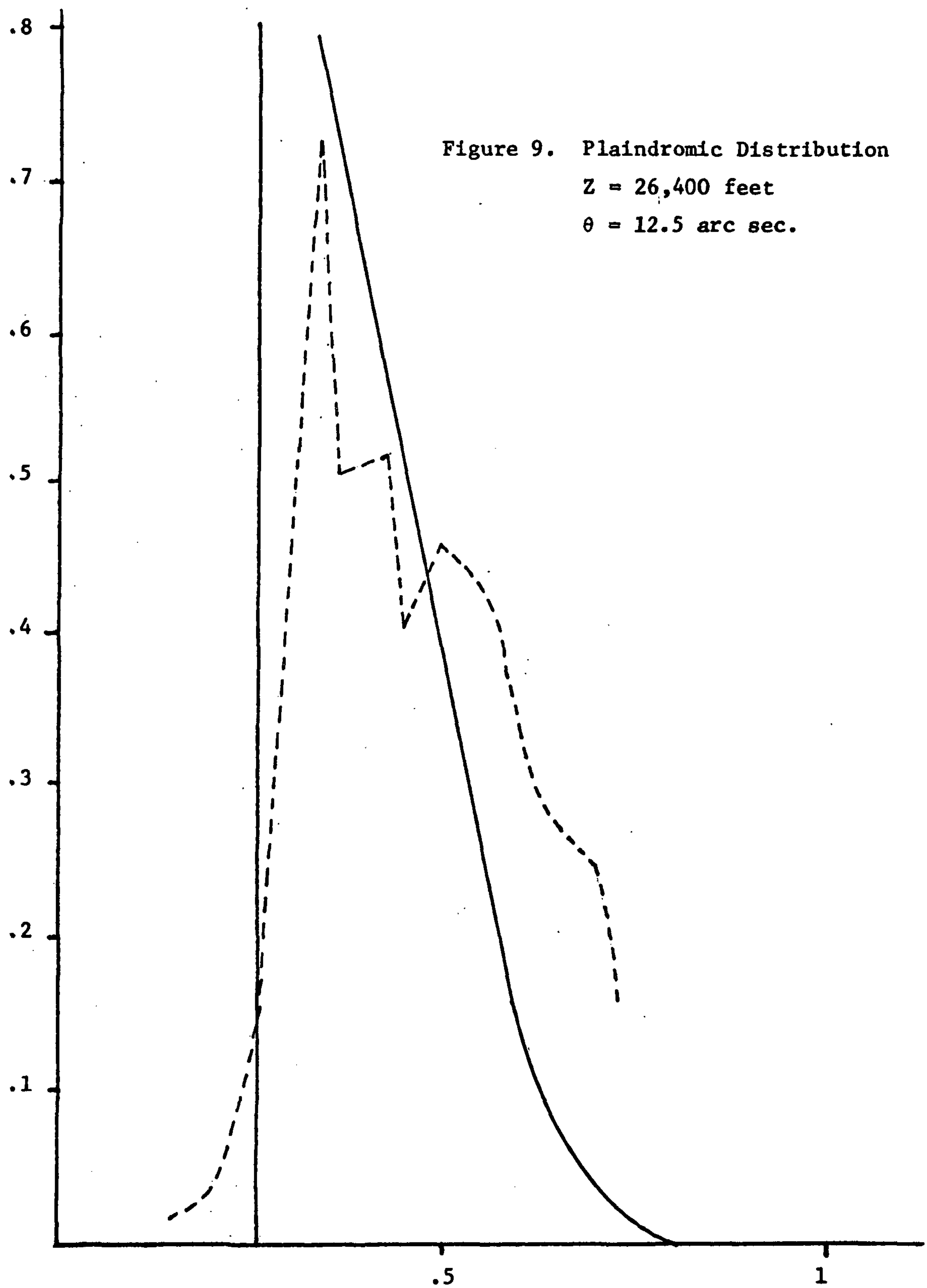

Figure 9. Plaindromic Distribution
Z = 26,400 feet
θ = 12.5 arc sec.

Figure 10. Plaindromic Distribution.

Z = 26,400 feet

θ = 25 arc sec.

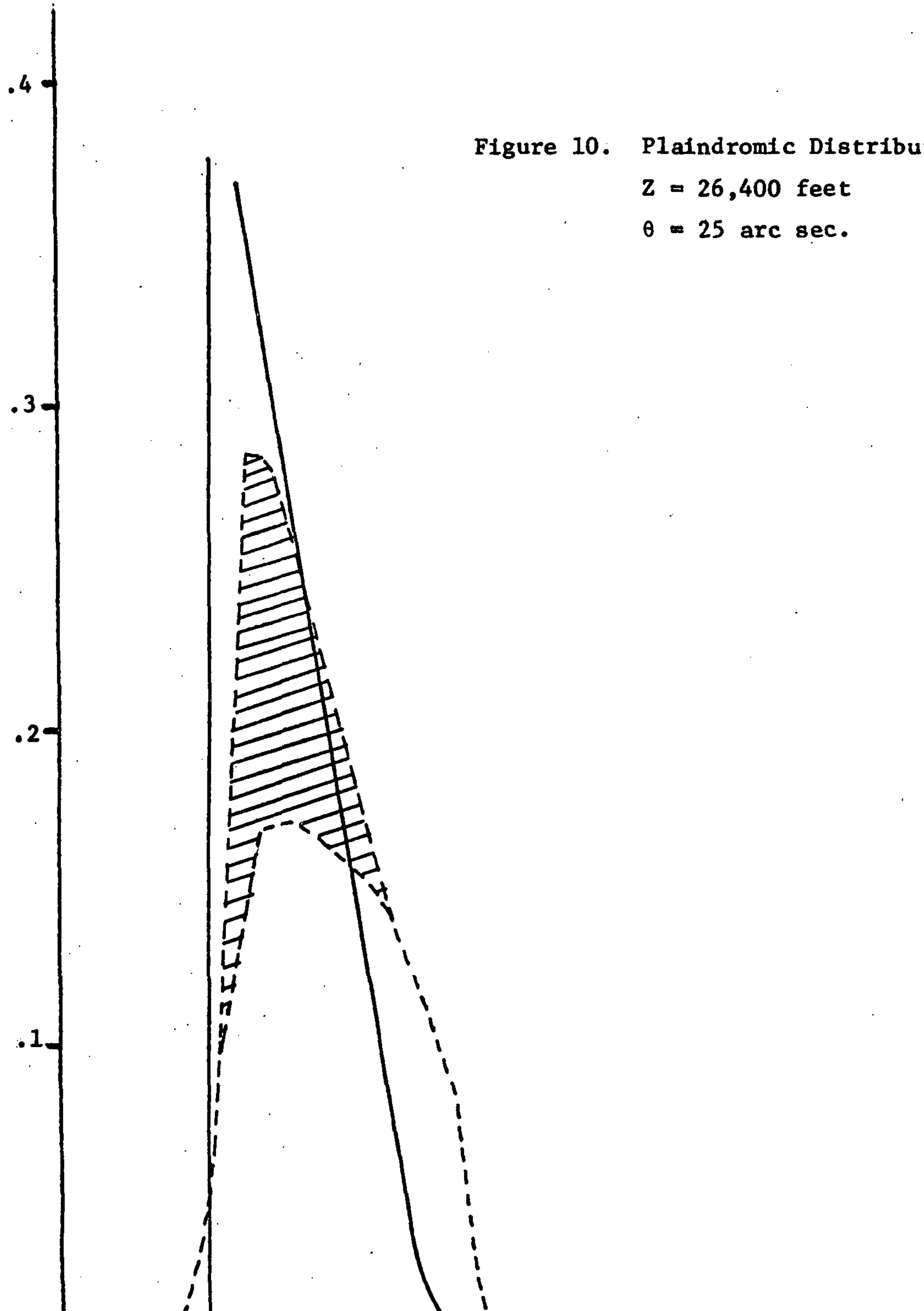

ATMOSPHERIC EFFECTS

In a previous section it was suggested that smearing of the transmitted beam by atmospheric turbulence might be sufficient to eliminate the central shadow. In order to estimate the magnitude of the atmospheric effects we may adopt a ray optics approach and consider a differential element of area in the transmitting aperture. A ray leaving this area will satisfy the ray equation

$$d(n\bar{s})/d\ell = \text{grad } n \tag{52}$$

where n is the index of refraction of the atmosphere, $\bar{s}$ is a unit vector tangent to the ray, and $d\ell$ is a differential element of path length along the ray. Integrating equation 52 along the optical path we obtain

$$n'\bar{s}' - n\bar{s} = \int_0^z (\text{grad } n)\, d\ell \tag{53}$$

For large path lengths the deviation of the ray will not depend on the value of the index of refraction at the end points. We may therefore set n and n' equal to unity and obtain

$$s' - s = \int_0^z (\text{grad } n)\, d\ell \tag{54}$$

The angular deviation of the ray is just proportional to the vector difference $s - \bar{s}'$. Following Chernov [9] we may obtain from equation 53, after some algebraic manipulations, the mean square deviation of the ray $\overline{\Delta\theta^2}$.

$$\overline{\Delta\theta^2} = \int_0^z \int_0^z dr_1 dr_2 \; (\text{grad}_1 \; \text{grad}_2 \; B(x_1-x_2, y_1-y_2, z_1-z_2)) \qquad (55)$$

B is the index of refraction correlation function which, for the Kolmogorov atmospheric model, is given by

$$B(r) = \int_{K_o}^{K_m} \frac{\Gamma(8/3)\,\sin(\pi/3)}{\pi} \, C_N^{\,2} \, \frac{\sin Kr}{r} \, K^{-8/3} \, dK \qquad (56)$$

where $C_N^{\,2}$ is the index of refraction structure constant and K_o, K_m are spatial frequencies corresponding to the outer and inner scales of turbulences (L_o, ℓ_o) respectively. Equation 56 may be substituted into equation 55 and the integrals performed to give [10]

$$\overline{\Delta\theta^2} = 5.7 \, C_N^{\,2} \, Z(\ell_o^{\,-1/3} - L_o^{\,-1/3}) \qquad (57)$$

Here $C_N^{\,2}$ and ℓ_o have been assumed to be constants, as would be the case for a horizontal path. For vertical paths the appropriate variation of $C_N^{\,2}$ and ℓ_o with altitude would have to be included. We will use the horizontal path expression and assume the maximum value of $C_N^{\,2}$ and a minimum value of ℓ_o in order to establish an upper limit on the amount of scattering by atmospheric turbulence which can be expected. Since L_o is much larger than L_o we may drop the last term of equation 57.

$$\overline{\Delta\theta^2} = 5.7\, C_N^{\,2}\, Z\, \ell_o^{-1/3} \tag{58}$$

The energy from a single differential element will be spread over an area whose size is of the order of σ, where σ is obtained directly by taking the product of the mean square scattering angle and the distance from the scattering center to the observation point and integrating over the entire optical path.

$$\sigma^2 = \int_o^z (z - \xi)^2 \left(\frac{d\,\overline{\Delta\theta^2}}{d\xi}\right) d\xi \tag{59}$$

This integration yields

$$\sigma^2 = 1.9\, C_N^{\,2}\, z^3\, \ell_o^{-1/3} \tag{60}$$

Equation 60 expresses the variance of a rays lateral displacement in the plane of the observation point. We now wish to determine the probability that a ray originating at a given point in the transmitter aperture will pass through the observation point. Since the phase fluctuations of a wave passing through the turbulent atmosphere are known to be normally distributed, it is therefore reasonable to assume that the angular deviations of the ray is also normally distributed. This conclusion could also be reached by considering that for propagation distances that are large compared to the inner scale of turbulence, the net angular deviation of a ray is the sum of a large number of small deviations. Hence appeal to the central limit thereon leads to a normal distribution. The lateral displacement of the ray is just the sum of the individual angular deviations, weighted by the lever arm, i.e., weighted by the distance from the scattering point to the observation point. Therefore, the lateral displacement of the ray is a random variable which is the sum of a number of independent gaussian random variables and hence should be normally distributed. While the foregoing arguments may not be absolutely rigorous they do indicate the reasonableness of a normal distribution. Under any circumstances the error introduced by assuming a normal distribution should not be great.

If we assume a gaussian distribution for the lateral ray displacements the contribution to the intensity at the observation point from a point (x_1,y_1) in the transmitting aperture is just

$$dI_{scatt} = \frac{|U_i(x_1y_1)|^2}{(2\pi)\ \sigma^2} \exp\{-\frac{x^2}{2\sigma^2}\}\ dx_1dy_1 \tag{61}$$

where x is the distance from the observation point to the point where the undeviated ray intersects the observation plane. If x_oy_o are the coordinates of the observation point then x^2 is given by

$$x^2 = (x_o - (1 + \frac{z}{R})x_1)^2 + (y_o - (1 + \frac{z}{R})y_1)^2 \tag{62}$$

The total scattered intensity is then given by

$$I_{scat} = \iint \frac{|U_1(x_1y_1)|^2}{(2\pi)\ \sigma^2} \exp\{-\frac{1}{2\sigma^2}[(x_o - (1 + \frac{z}{R})x_1)^2+(y_o - (1 + \frac{z}{R})y_1)^2]\}dx_1dy_1 \tag{63}$$

where the integration extends over the unobscured portion of the aperture.

To simplify our calculations let us assume an aperture illuminated by a beam of uniform intensity. We will also restrict ourselves to consideration of observation points on the optical axis of the transmitting telescope. With these restrictions equation 63 becomes on changing to polar coordinates

$$I_{scat} = \frac{1}{\sigma^2} \int_a^b \exp \{- \frac{1}{2\sigma^2} (1 + \frac{z}{R})^2 r_1^2\} r_1 dr_1 \tag{64}$$

$$I_{scat} = (R/(z + R))^2 [\exp \{-(1 + \frac{z}{R})^2 \frac{a^2}{2\sigma^2} \} - \exp \{-(1 + \frac{z}{R})^2 \frac{b^2}{2\sigma^2}] \tag{65}$$

Equation 65 may be evaluated numerically to give an estimate of the amount of filling of the central shadow. If we assume strong turbulence we may take C_N^2 to be on the order of 10^{-7} meters$^{-1/3}$ and the inner scale of turbulence to be about 1 mm. With these values σ is found to be 1.5 m^2. If we then assume a 25 arc second beam and a range of 20 Km, we find that the intensity on the optical axis is about 2% of the intensity in the transmitting aperture. Thus under the assumed conditions the beam smearing would be appreciable. For weak turbulence, however, C_N might be as small as 10^{-9} meters$^{-1/3}$, in which case the on axis intensity is only

$$(\frac{1}{25} e^{-830})$$

times the intensity in the aperture. Clearly for weak turbulence the spreading of the beam is entirely negligible. It should be remembered that these calculations apply only to a horizontal range since the altitude profile of C_N^2 and ℓ_o have been neglected. For vertical paths the beam smearing will be much less since a C_N^2 decreases and ℓ_o increases with altitude.

CONCLUSIONS

The calculated beam profiles indicate that for the ranges and size optics to be used on the MSFC-AVLOC experiment the central shadow of the cassegrainian secondaries will be very dark and hence on axis operation will be impossible unless provisions are made to eliminate the shadow. Diffraction of light into the shadow was found to be negligble and the bright central spot, while present and strong, is far to small to be of any practical use.

Smearing of the beam by atmospheric turbulence has also been considered but it was found that except for very long, horozontal paths and strong turbulence conditions the effect would be small.

REFERENCES

1. "High Altitude Aircraft Experiment Test for Visible Laser Optical Communications" Astrionics Laboratory, Marshall Space Flight Center, Internal Document, August 1970

2. McIntyre, C. M., "Far Field Pattern of Defocused Telescope" Perkin Elmer Engineer Report No. 10798, Norwalk Conn., Sept. 1971

3. Goodman, J. W. "Introduction to Fourier Optics" McGraw Hill, San Francisco, (1968)

4. Watson, G. N. A Treatise on the Theory of Bessel Functions Cambridge University Press. (1966)

5. Abromawitz, M. and I. A. Segun Handbook of Mathmatical Functions Dover, New York.

6. Born, M. and E. Wolf "Principles of Optics" Page 375, Pergamon Press, London (1965)

7. Peters, W. N. and A. M. Ledger Applied Optics 9, Page 1435, (1970)

8. Dey, K. K. and P. Khastgir Comments on the Calculated Radiation Patterns of Truncated Gaussian Aperture Distribution, IEEE Trans, Antenna and Propagation, AP-19, 785 (1971)

9. Chernov, L. A. "Wave Propagation in a Random Medium", McGraw-Hill, New York, 1960.

10. Chiba, T., Spot Dancing of a Laser Beam Propagated Through the Turbulent Atmosphere, Appl. Optics. 10, 2456, 1971

APPENDIX A

COMPUTER PROGRAMS

1. Near Field Diffraction Pattern

This program computes the near field diffraction pattern of a circular aperture or obstructed circular aperture by direct numerical evaluation of the Fresnel diffraction integral. A double precision Simpson's Rule integration is used to evaluate the integral. The program as listed below will allow the aperture to be illuminated with a beam of arbitrary divergence angle and either uniform, gaussian or plaindromic gaussian intensity profile. A later modification will also accept a displaced gaussian beam.

Input to the program consists of three data cards. The first card specifies the type of field distribution which is to be used, i.e., gaussian, plaindromic, or uniform, beginning in column one. The first character is compared with the characters 'G', 'P' and 'U' stored in an array TCLASS and a branching flag is set and passed to the subroutine FRES*8 via the labled common block /TYPE/. If the first character is other than 'G', 'P' or 'U' an error message is generated and execution terminates. The second data card contains the diameter of the obscuration (which may be zero), the diameter of the aperture in inches, the beam power in watts and the wavelength in angstrom units. The card format is 4F10.4. The third data card contains the range, in feet, the beam width parameter in inches, the beam divergence angle in arc seconds, the distance off axis of the first field point to be computed and the interval at which field points are to be spaced, both in feet, the number of field points to be calculated and the number of points to be used in the Simpson's Rule integration.

The input parameters are printed in the output listing and are then converted to metric units. The number of points specified for the Simpson's Rule algorithm is also checked and if it is even, it is increased by one.

The subroutine DSMPC is called twice to compute the real and imaginary parts of the Fresnel Diffraction integral for the first field point. The intensity is then computed by taking the absolute square of the field. The off axis distance of the field point is then incremented and the intensity at the next field point computed. This process is continued until the specified number of field points have been calculated.

After one profile has been calculated the program reads a new data card which may modify the range, beam width, beam divergence, field point and/or number of points in the integration. Execution continues until all data is exhausted.

```
// EXEC FORTGCLG,PARM.FORT='LIST,NAME=AVGO',
//  COND.GO=ONLY   SUPPRESS GO STEP
//FORT.SYSIN DD *
C     PROGRAM TO COMPUTE FRESNEL DIFFRACTION PATTERN OF A CIRCULAR
C     APERTURE  WITH A CENTRAL OBSCURATION
C     USING A DOUBLE PRECISION SIMPSON RULE WITH CORRECTOR TERMS
C
C
C     A        = DIAMETER OF OBSCURATION   INCHES
C     B        = DIAMETER OF APERTURE      INCHES
C     LAMBDA   = WAVELENGTH                ANGSTROM UNITS
C     W        = WIDTH OF GAUSSIAN BEAM    INCHES
C     POWER    = LASER POWER               WATTS
C     Z        = RANGE                     FEET
C     RHO      = DISTANCE OFF AXIS         FEET
C     THETA    = BEAM DIVERGENCE           ARC SECONDS
C     NPTS     = NUMBER OF POINTS IN INTEGRATION
C
C     T        = TRUNCATION POINT FOR PLAINDROMIC FIELD
C
      EXTERNAL FRES
      COMMON W,K,RHO,PI,TWOPI,R,Z,NTYP
      COMMON/TYPE/PASSA,PASSB,T,WI,IDIST
      DIMENSION LINE (80)
      INTEGER TCLASS(3)/'U','G','P'/,TNUM/3/
      REAL*8 A,B,POWER,LAMBDA,PI,TWOPI,K,Z,W,THETA,R,RHO,RHO1,DRHO,RMAX,
     *SSM,SCM,E1,E2,INT
     *,PASSA,PASSB,T,WI
      PI = 3.141592653589793D0
      TWOPI=2.0D0 * PI
C     READ FIELD DISTRIBUTION TYPE AND SET BRANCHING FLAG
      READ(5,908) LINE
      IDIST=0
      DO 3 KK=1,TNUM
      IF(LINE(1).EQ.TCLASS(KK))  IDIST=KK
    3 CONTINUE
      IF(IDIST.EQ.0)  GO TO 10
      IF(IDIST.NE.3)  GO TO 11
      READ(5,911) T,WI
      WI=1.2700025D-02 * WI
      T=1.2700025D-02 * T
   11 CONTINUE
C     READ PARAMETERS AND CONVERT UNITS
      READ(5,901) A,B,POWER,LAMBDA
      WRITE(6,902)  A,B,POWER,LAMBDA
      A=1.2700025D-02 * A
      B=1.2700025D-02 * B
      PASSA=B-A
```

```
      PASSB=B
      K=2.0D10 * PI / LAMBDA
    1 READ(5,903,END=800) Z,W,THETA,RHO1,DRHO,NRHO,NPTS
      WRITE(6,904) Z,W,THETA
      WRITE(6,909) LINE
      W=1.2700025D-02 * W
      Z=0.3048006096D0 * Z
      THETA = 4.84814D-06 * THETA
      R = W/THETA
      RHO1 = 0.3048006096D0 * RHO1
      DRHO = 0.3048006096D0 * DRHO
C
C     PARAMETERS HAVE BEEN CONVERTED TO METRIC UNITS
C     NOW CHECK NUMBER OF POINTS *** IT MUST BE ODD
C
      N=MOD(NPTS,2)
      IF(N.EQ.0) NPTS=NPTS+1
      WRITE(6,906) NPTS
      DO 2 J=1,NRHO
      RHO = RHO1 + (J-1)*DRHO
      NTYP=1
      CALL DSMPC(SSM,FRES,E1,NPTS,A,B)
      NTYP=2
      CALL DSMPC(SCM,FRES,E2,NPTS,A,B,)
C     COMPUTE INTENSITY
      INT=((K/Z)**2)*((2.0D0*POWER)/(PI*(W**2))*(SCM**2+SSM**2)
C     PRINT RESULTS
    2 WRITE(6,907) RHO,INT,E1,E2
      GO TO 1
   10 WRITE(6,910)
  800 STOP
  901 FORMAT(4F10.4)
  902 FORMAT('1',25X,'PARAMETER LIST'//10X,'A=',F10.5,'INCHES',5X,'B=',
     *F10.2,' INCHES'/10X,'POWER=',F6.2,' WATTS'/10X,'WAVELENGTH=',F8.2,
     *' ANGSTROMS '      )
  903 FORMAT(5D14.6,2I5)
  904 FORMAT(10X,'RANGE=',F12.2,' FEET'/10X,'BEAM WIDTH=',F10.2,' INCHES
     *'/10X,'BEAM DIVERGENCE=',F10.2,' ARC SECONDS')
  906 FORMAT(10X,'USING A ',I5,' POINT SIMPSONS RULE ')
  907 FORMAT('0',15X,'DISTANCE OFF AXIS =',F10.4,/5X,'INTENSITY =',
     *D24.16/25X,'ERROR TERMS',5X,2D26.16)
  908 FORMAT(80A1)
  909 FORMAT(10X,'TYPE DISTRIBUTION = ',80A1)
  910 FORMAT('  ILLEGAL FIELD DISTRIBUTION SPECIFIED    EXECUTION TERMIN
     *ATED')
  911 FORMAT(2F10.4)
      END
```

The subroutine DSCMP is a double precision Simpson's Rule Algorithm with two correction terms. The correction terms are printed to provide an estimate of the accuracy of the integration routine.

```
      SUBROUTINE DSMPC(SUM,FUN,E,N,FLL,FUL)
      DOUBLE PRECISION SUM,S1,S2,S3,S4,FN,FLL,FUL,DX X,FJ,Y,E,FUN
      S1 = 00.0D0
      S2 = 00.0D0
      S3 = 00.0D0
      S4 = 00.0D0
      FN = N-1
      DX = (FUL-FLL)/FN
      DO 10 I=1,N
      J=I-1
      FJ=J
      X=DX*FJ  +FLL
      Y=FUN(X)
      IF(I.EQ.1.OR.I.EQ.N) GO TO 1
      IF(I.EQ.2.OR.I.EQ.(N-1)) GO TO 2
      K=MOD(I,2)
      IF(K) 3,4,3
    1 S1=S1+Y
      GO TO 10
    2 S2=S2+Y
      GO TO 10
    3 S3=S3+Y
      GO TO 10
    4 S4=S4+Y
   10 CONTINUE
      SUM=(S1+4.0D0*(S2+S4) + 2.0D0*S3) * (DX/3.0D0)
      E=(-4.0D0*S1 + 7.0D0*S2 + 8.0D0*(S4-S3) + FUN(FLL-DX    ) + FUN(
     1 FUL+DX)) * (DX/(-9.0D1))
      SUM=SUM+E
      RETURN
      END
//LKED.SYSLMOD DD DSNAME=UA0L02.EEG00118.PWRFLW(AVLOC2),DISP=SHR,
// UNIT=DISK,VOL=SER=UA0L02,SPACE=
//GO.SYSIN DD *  PROGRAM CHECKOUT DATA

GAUSSIAN
    8.0000   24.0000    1.0000 4880.0000
 80.000000D 03 24.000000D 00  1.500000D 02  1.000000  00  1.000000D 00    1     31
```

The subroutine FRES*8 is called by DSMPC to compute the integrand. Two Bessel function approximations are used; a Jacobi asymptotic expansion and an ascending power series. The program selects the appropriate routine each time depending on the value of the argument.

```
      REAL FUNCTION FRES*8(R)
      REAL*8 W,K,R,RHO,Z,ARG,A,A2,A3,A4,A5,P,Q,PI,TWOPI,RND,ARGJ,JZRO,
     *TRIG,RAD
     *,A6,A7,FAC,XI
     *,U,ARGE,ARGRT,PASSA,PASSB,T
     *,WI
      COMMON W,K,RHO,PI,TWOPI,RAD,Z,NTYP
      COMMON/TYPE/PASSA,PASSB,T,WI,ITYP
C     COMPUTE ZERO ORDER BESSEL FUNCTION FOR LARGE ARGUMENT USING
C         JACOBI ASYMPTOTIC EXPANSION
C
      ARGJ=K*R*RHO/Z
      IF(ARGJ.LT.1.0D01) GO TO 1
      A=8.0D0*ARGJ
      A2=A*A
      A3=A*A2
      A4=A*A3
      A5=A*A4
      A6=A*A5
      A7=A*A6
      P=1.0D0 - 4.5D0/A2 + 4.59375D2/A4 - 1.50077812 D05/A6
      Q=1.0D0/A - 3.75D1/A3 + 7.441875D3/A5 - 3.62 3071875D06/A7
      RND=ARGJ/TWOPI
      NR=RND
      RND=NR
      RND=ARGJ-RND*TWOPI
      RND = RND-PI/4.0D0
      JZRO=DSORT(2.0D0/(PI*ARGJ))*(P*DCOS(RND) + Q*D IN(RND))
    3 CONTINUE
      ARG=0.5D0*K*(1.0D0/RAD + 1.0D0/Z)*(R**2)
      IF(NTYP.EQ.1) TRIG=DSIN(ARG)
      IF(NTYP.EQ.2) TRIG=DCOS(ARG)
      GO TO (11,12,13),ITYP
   11 FRES=TRIG*JZRO*R/1.414213562373095D0
      RETURN
   12 CONTINUE
      FRES = DEXP(-1.0D0*((R/W)**2)) * TRIG * JZRO 8
      RETURN
   13 ARGE=-1.0D0*(((PASSB-R)/PASSA)*(T/WI))
      ARGRT=(PASSB-R)/R
      IF(ARGRT.LE.0.0D0) GO TO 14
      FRES=DEXP(ARGE)*JZRO*R*DSQRT(ARGRT)*TRIG*W*T/( I*PASSA)
      RETURN
```

```
14 FRES=0.0D0
   RETURN
 1 A= -1.0D0 * (ARGJ/2.0D0)**2
   AL=1.0D0
   FAC=1.0D0
   JZRO=1.0D0
   DO 2 I=1,20
   XI=I
   FAC=FAC*XI
   A1=A1*A
   A3=A1/(FAC**2)
   A4=DABS(A3)
   IF(A4.LT.1.0D0-16) GO TO 3
   JZRO=JZRO + A3
 2 CONTINUE
   GO TO 3
   END
```

2. Program for Calculation, Field Intensity on Axis

This program evaluates the Fresnel diffraction integral for field points on the optical axis. In addition, it computes the field distribution from the geometrical optics approximation.

```
   PI=3.14159
 4 READ (5,1) A,B,W,P,WAVE,THETA,Z
   WRITE(6,2) A,B,W,P,WAVE,THETA,Z
   A=0.0127*A
   B=0.0127*B
   W=0.0127*W
   WNUM=2.0E10*PI/WAVE
   Z=0.3048*Z
   R=W/(4.848E-06*THETA)
   C=2.0*P/(PI*(W**2))
   D=(1.0+Z/R)**2 + ((2.0*Z)/(WNUM*(W**2)))**2
   C=C/D
   X=(A/W)**2
   Y=(B/W)**2
   ARG=(WNUM/2.0)*(A*A-B*B)*(1.0/Z+1.0/R)
   PD=C*(EXP(-2.0*X) + EXP(-2.0*Y) - 2.0*EXP(-1.0 (X+Y))*COS(ARG))
   WRITE(6,.3) PD
   WRITE(6,13)
   RAT=(R+Z)/R
   XW=W*RAT
   CO=(2.0*P)/PI*(XW**2))
```

```
      XLO=A*RAT
      XHI=B*RAT
      WRITE(6,11) XLO,XHI
      DX=(XHI-XLO)/10.0
      DO 10 I=1,11
      X=(I-1)*DX + XLO
      PD=CO*EXP(-2.0*(X/XW)**2)
   10 WRITE (6,12) X,PD
   11 FORMAT(10X,'LIMITS OF GEOMETRICAL SHADOW ',25 4.6)
   12 FORMAT(20X,'X= 'E14.6,' INTENSITY= ',E14.6)
   13 FORMAT('0 GEOMETRICAL OPTICS APPROCIMATION')
      GO TO 4
    1 FORMAT(6F10.4,F10.0)
    2 FORMAT('0',10X,6F10.4/11X,F10.0)
    3 FORMAT(10X,'INTENSITY = ',E12.4,' WATTS PER METER SQ ')
      END
```